Cancer-associated fibroblast-derived interleukin-1β mediates pro-tumor CCL22 signaling in head and neck cancer

Yu-Hsuan, Huang[a, #], Che-Ying Chang[a,#], Yi-Zih Kuo[b], Wei-Yu Fang[c], Hung-Ying Kao[d], Sen-Tien Tsai[b,e,*], and Li-Wha Wu[a,f,*]

[a]Institute of Molecular Medicine, College of Medicine, National Cheng Kung University, Tainan, Taiwan, R.O.C.

[b]Department of Otolaryngology, College of Medicine, National Cheng Kung University, Tainan, Taiwan, R.O.C.

[c]Institute of Basic Medical Sciences, College of Medicine, National Cheng Kung University, Tainan, Taiwan, R.O.C.

[d]Department of Biochemistry, School of Medicine, Case Western Reserve University, Cleveland, OH, U.S.A.

[e]Cancer Center, National Cheng Kung University Hospital, Tainan, Taiwan, R.O.C.

[f]Department of Laboratory Science and Technology, College of Health Sciences, Kaohsiung Medical University, Kaohsiung, Taiwan, R.O.C.

#, equal contribution

*, corresponding authors

Please address correspondence to:

Li-Wha Wu, Institute of Molecular Medicine, College of Medicine, National Cheng Kung University, Tainan, Taiwan, R.O.C. Tel:+886-6-2353535 ext. 3618; Fax:+886-6-2095845; E-mail: liwhawu@mail.ncku.edu.tw; Sen-Tien Tsai, Department of Otolaryngology, College of Medicine, National Cheng Kung University, Tainan, Taiwan, R.O.C. Tel:+886-6-2353535 ext.5311; E-mail: T602511@mail.ncku.edu.tw.

Supporting methods

Reverse transcription followed by quantitative polymerase chain reaction (RT-qPCR)

Total RNA was isolated from snap-frozen tissues or mouse tumor tissues using TRIZOL reagent. One microgram of total RNA was reverse transcribed into cDNA in 20 μl with random hexamers, oligo-dT primers, and MMLV enzyme. Quantitative PCR was conducted using StepOne^{TM} Real-Time PCR System (Applied Biosystems, Waltham, MS, USA). All reactions were performed in triplicate, and the relative expression of mRNA was calculated using $2^{-\Delta CT}$ method with *RNA28S*, *ACTB* or *Gapdh* as the reference. All primer sequences were listed in Table S1.

Cell culture

CAL-27, HEK-293 and A549 cells from Biosource Collection and Research Center (BCRC) were passaged for less than six months after resuscitation. The origin and identity of TW2.6, OC-2, OC-3, and OEC-M1 were authenticated by DNA (STR)

profiling by BCRC. CAL-27 and HEK-293T cells were cultured in Dulbecco's Modified Eagle's medium (DMEM) with 10% heat-inactivated FBS, 100 units/ml penicillin and 0.1 mg/ml streptomycin (antibiotics). TW2.6 cells were cultured in the mixture of F12 and DMEM (1:3) supplemented with 10% heat-inactivated FBS and antibiotics. OC-3 cells were maintained in a mixture of DMEM and KSFM (1:2) supplemented with 10% heat-inactivated FBS and antibiotics. OEC-M1 were cultured in RPMI1640 with 10% heat-inactivated FBS and antibiotics. Murine oral cancer line, AT-84, was propagated as described (1). A549 cells were maintained in MEM plus 10% heat-inactivated FBS, non-essential amino acids, sodium pyruvate, and antibiotics.

Lentiviral preparation

For gene silencing, control sh*Luc*, *CCL22* shRNA (human) or *Ccl22* shRNA (mouse) expressing plasmids were individually transfected into HEK-293T cells by using Lipofectamine 2000. The shRNA clone numbers and their sequences were listed in Table S2. Viral particles in the medium were collected 48 hours after infection. The titer was measured by using the half maximal inhibitory concentration of A549 cells. CAL-27 or TW2.6 were used as hosts for *CCL22* depletion. For *CCL22* overexpression, we established a stably integrated vector or Flag-tagged CCL22 clones in Ca9-22 and OC-3 lines by the infection of the lentiviruses bearing the pLKO-AS2 vector or pLKO-AS2-Flag-CCL22. The stable clones were selected by puromycin (1 mg/ml).

Doubling tim*e*

Cells were seeded at 10% confluency in culture medium in 24-well plates and infected with sh*CCL22* expression lentivirus. After infection, cell numbers in experimental groups were counted daily for 3-4 days.

Wound-healing assay

Cells were seeded at 80% confluency in culture medium in 6-well plates coated with 5 μg/mL collagen. Following viral infection, confluent cells were treated with mitomycin C for 24 hours to stop cell proliferation. Scratches were made by 200-microliter loading tips. Cell migration was monitored and photographed at 0-42 hours post-wounding, depending on the cell types. The mean distance of ten wound width along the wound at different time points was measured, and the migration rate was presented as the migrating distance per hour.

Matrigel invasion Assay

Cells (3×10^5/well) were added in triplicate to upper chambers with 8-μm-pore polycarbonate membranes coated with 100 μg of Matrigel (BD Biosciences, Bedford, MA, USA) in 24-well Millicell culture inserts. Lower chambers were filled with 500 μL of growth medium. After 6–24 hours incubation, the cells that migrated to the lower surface were stained with Giemsa solution and counted in high power fields under a microscope. This assay was independently repeated two times.

Drug-induced oral cancer mouse model

To mimic the etiology of oral cancer among Southeast Asian and Taiwanese patients with betel quid chewing habits, we used a previously established mouse model (2). Male C57BL/6 mice were randomized into two groups (4-5 mice per group): the control group received only drinking water with the PEG solvent; the treatment group received both 100 μg/mL 4-nitroquinoline 1-oxide (4-NQO; *Alfa Aesar, Ward Hill, MS, USA*) and 500 μg/mL arecoline hydrobromide (Tokyo Chemical Industry, Tokyo, Japan) for 12 weeks. Regular sterilized drinking water was resumed until week 28. Precancerous and cancerous lesions of the tongue were recorded and photographed monthly started at week five post-treatment. The mice were sacrificed at the end of 28 weeks, and tissues collected.

Tissue collection

Blood samples were collected via a tail artery, and then cervical dislocation was performed at the time of sacrifice. We also excised tongues, spleens and the cervical lymph nodes. Half of the tongue tissues were immediately snap-frozen for total RNA isolation, and the remaining halves were fixed with 10% formalin and embedded in paraffin and sliced into 4 μm-thick sections for hematoxylin and eosin staining.

Isolation of immune cells by flow cytometry

The Mouse Regulatory T cell Staining Kit #3 (eBiosciences, San Diego, CA, USA) was

used to measure the percentage of Tregs in peripheral blood, spleen and cervical lymph nodes in a drug-induced oral cancer model. Following centrifugation of 200 μl of whole heparinized blood in Histopaque-1083 (Merck, Darmstadt, Germany), isolated peripheral blood mononuclear cells (PBMCs) were washed with PBS containing 2% of BSA and resuspended in flow cytometry staining buffer (FSB). Following meshing spleens and cervical lymph nodes through 40- and 70-μm cell strainers, respectively, the samples were rinsed with red blood cell lysis buffer (Merck, Darmstadt, Germany), resuspended in FSB, and stained at 4°C in the dark for 30 min with the cocktail of anti-mouse CD4 FITC and CD25 PE antibodies (Table S3). The intracellular staining of FOXP3 was performed in the 1X permeability buffer using the anti-mouse FOXP3-PE-Cy5 or isotype control (Table S3). All flow cytometry experiments were performed and analyzed on the flow cytometer FACs Canto (BD Biosciences) equipped with laser lights (405 nm, 488 nm, and 633 nm).

Fibroblast isolation and subculture

Fibroblasts from patient oral cancer specimens were isolated as described (3). Briefly, small pieces of connective tissues (1x1x1 mm^3) were maintained in DMEM containing 10% FBS and antibiotics following saline washes and removal of epithelial tissues. Once the cells reach confluence, epithelial cells were removed by brief trypsinization. The remaining cells were mostly fibroblasts. In addition to vimentin positivity and E-

cadherin negativity, we also confirmed spindle-like morphology by microscopy and the expression of alpha-smooth muscle actin (αSMA) and fibroblast-specific protein 1 (FSP1) in isolated fibroblasts by Western blot analysis.

Collection of conditioned medium

The conditioned medium (CM) was collected from cancer-associated fibroblasts (CAF) after 24-48 hours of incubation in serum-free medium and concentrated through Vivaspin 6 tubes (GE Healthcare, Chicago, IL, USA) and stored at -80 °C. To determine the importance of CAF-derived IL-1β, sh*Luc*- or sh*IL1B*-infected fibroblasts were enriched by puromycin and cultured in the regular medium. Following 24 hours of incubation, the medium was removed and replaced with a serum-free culture medium and CM was collected after another 24 hours of incubation.

Enzyme-linked immunosorbent assay (ELISA) for CCL22

The abundance of CCL22 protein in CM was quantified by using DuoSet (R&D Systems, Minneapolis, MN, USA) according to the supplier's instructions. The detection limit for CCL22 protein was 7.81 pg/mL.

In vitro Treg Migration Assays

Following the isolation of human Treg from human peripheral blood with informed consent by MACSxpress® Whole Blood Treg isolation kit as described (Miltenyi Biotec, Bergisch Gladbach, Germany), the indicated oral cancer cells were for 3 days

with or without CAF-CM. The co-culture medium was collected as described in the CM preparation. A total of 5×10^4 sorted Treg cells were added in 100 μl to the upper chamber of a 24-well Transwell plate with a 5um insert (Millipore). The lower wells contained CM from cancer cells treated with or without CAF. The number of Treg cells that migrated to the lower well after 4-hr incubation was counted with a hemocytometer. Each experiment was performed in triplicate.

Supporting Tables and Figures

Table S1. Primer list

Table S2. ShRNA clones and sequences

Table S3. Antibody list

Fig. S1. The mRNA expression of *CCL17* and *CCL22* in the head and neck cancer patient cohorts from the ONCOMINE database.

Fig. S2. Little or no significant correlation between *CCL22* expression and the overall and recurrence-free survival.

Fig. S3. Differential expression of CCL22 protein in oral cancer cell lines

Fig. S4. The abundance of CCL22 protein in the CM isolated from CCL22-knockdown cells.

Fig. S5 Concordant decrease of *Foxp3* mRNA with *Ccl22* mRNA expression in *Ccl22* knockdown tumor grafts.

Fig. S6. The induction of mouse oral cancer by 4NQO and arecoline.

Fig. S7. CM derived from CAF-treated oral cancer cells promoted Treg migration and mRNA expression of *TGFB, IFNG, and MCP1* in isolated NFs and CAFs derived from clinical specimens.

Fig. S8. Recombinant IL-1β stimulates CCL22 mRNA expression in oral cancer cells.

Fig. S9. The NF-κB subunit, p65 potently induces *CCL22* promoter activity.

Fig. S10. The status of activating phosphorylation of NF-κB proteins in pairwise NFs and CAFs.

Reference

1. Lou E, Kellman RM, Hutchison R, Shillitoe EJ. Clinical and pathological features of the murine AT-84 orthotopic model of oral cancer. Oral Dis. 2003;9(6):305-12.

2. Chang NW, Pei RJ, Tseng HC, Yeh KT, Chan HC, Lee MR, et al. Co-treating with arecoline and 4-nitroquinoline 1-oxide to establish a mouse model mimicking oral tumorigenesis. Chem Biol Interact. 2010;183(1):231-7.

3. Liu Y, Hu T, Shen J, Li SF, Lin JW, Zheng XH, et al. Separation, cultivation and biological characteristics of oral carcinoma-associated fibroblasts. Oral Dis. 2006;12(4):375-80.

Table S1 Primer list

Primer	Sequence
CCL22-F	5’-CGTGG TGAAA CACTT CTACT G-3’
CCL22-R	5’-TCGGC ACAGA TCTCC TTATC-3’
CCR4-F	5’-TGCCT CACAG ACCTT CCTC-3’
CCR4-R	5’-GCCTT GATGC CTTCT TTGG-3’
FOXP3-F	5’-CACTG CTGGC AAATG GTGTC-3’
FOXP3-R	5’-TGGCA GTGCT TGAGG AAGTC-3’
IL1B-F	5’-CCTGT TGTCT ACACC AATGC-3’
IL1B-R	5’-GGTTG CTCAT CAGAA TGTGG-3
RNA28S-F	5’-CGAAT ACAGA CCGTG AAAGC-3’
RNA28S-R	5’-GATAG GAAGA GCCGA CATCG-3’
ACTB-F	5’-ACTCTTCCAGCCTTCCTTCC-3’
ACTB-R	5’-CTCGTCATACTCCTGCTTGC-3’
TGFB-F	5’-ACATTGACTTCCGCAAGGAC-3’
TGFB-R	5’-CCGGGTTATGCTGGTTGTA-3’
IFNG-F	5’-CTGTTACTGCAGGACCCAT-3’
IFNG-R	5’-TCCGCTACATGTGAATGACC-3’
MCP1-F	5’-GCCTCCAGCATGAAAGTCTC-3’
MCP1-R	5’-AGGTGACTGGGGCATTGAT-3’
Ccl22-F	5’-GACTA CATCC GTCAC CCTCT-3’
Ccl22-R	5’-AGTAG CTTCT TCACC CAGAC C-3
Foxp3-F	5’-TACCA CAATA TGCGA CCCCC-3’
Foxp3-R	5’-GGCGA ACATG CGAGT AAACC-3’
Il1b-F	5’-GTCGC TCAGG GTCAC AAGAA-3’

Table S1 Primer list (Continued)

Primer	Sequence
Il1b-R	5’-GTGCT GCCTA ATGTC CCCTT-3’
Gapdh-F	5’-TGTCA AGCTC ATTTC CTGGT-3’
Gapdh-R	5’-TAGGG CCTCT CTTGC TCAGT-3’

Table S2 ShRNA clones and sequences

Name	Clone ID	Sequence (5'-->3')
Human		
sh*CCL22* #1	TRCN0000371675	ATGTTGCTGACACCCAGAAAG
sh*CCL22* #2[a]	TRCN0000058001	GCTAACCTTCAGGGATAAGGA
Mouse		
sh*Ccl22* #1[a]	TRCN0000067833	GCTCAGAATCAGATTTCTTAA
sh*Ccl22* #2	TRCN0000067834	GCTACTCCATAAACTGTCCTA

a, clones used for in vivo tumorigenesis

Table S3 Antibody list

Antibodies	Cat. No. (Company)	Application
Alexa Fluor® 647 anti-human CD194 (CCR4)	359403 (BioLegend)	Flow
Alexa Fluor® 647 Mouse IgG1, κ Isotype Ctrl (FC)	400130 (BioLegend)	Flow
Anti-MDC antibody (CCL22)	ab9847 (Abcam)	WB
Anti-FOXP3 antibody	ab22510 (Abcam)	WB
Anti-Mouse CD4 FITC	11-0042 (eBioscience)	Flow
Anti-Mouse CD25 PE	12-0251 (eBioscience)	Flow
Anti-Mouse/Rat Foxp3 PE-Cy5	15-5773 (eBioscience)	Flow
Rat IgG2a κ Isotype Control PE-Cy5	15-4321 (eBioscience)	Flow

Fig. S1 The mRNA expression of *CCL17* and *CCL22* in the head and neck cancer patient cohorts from the ONCOMINE database

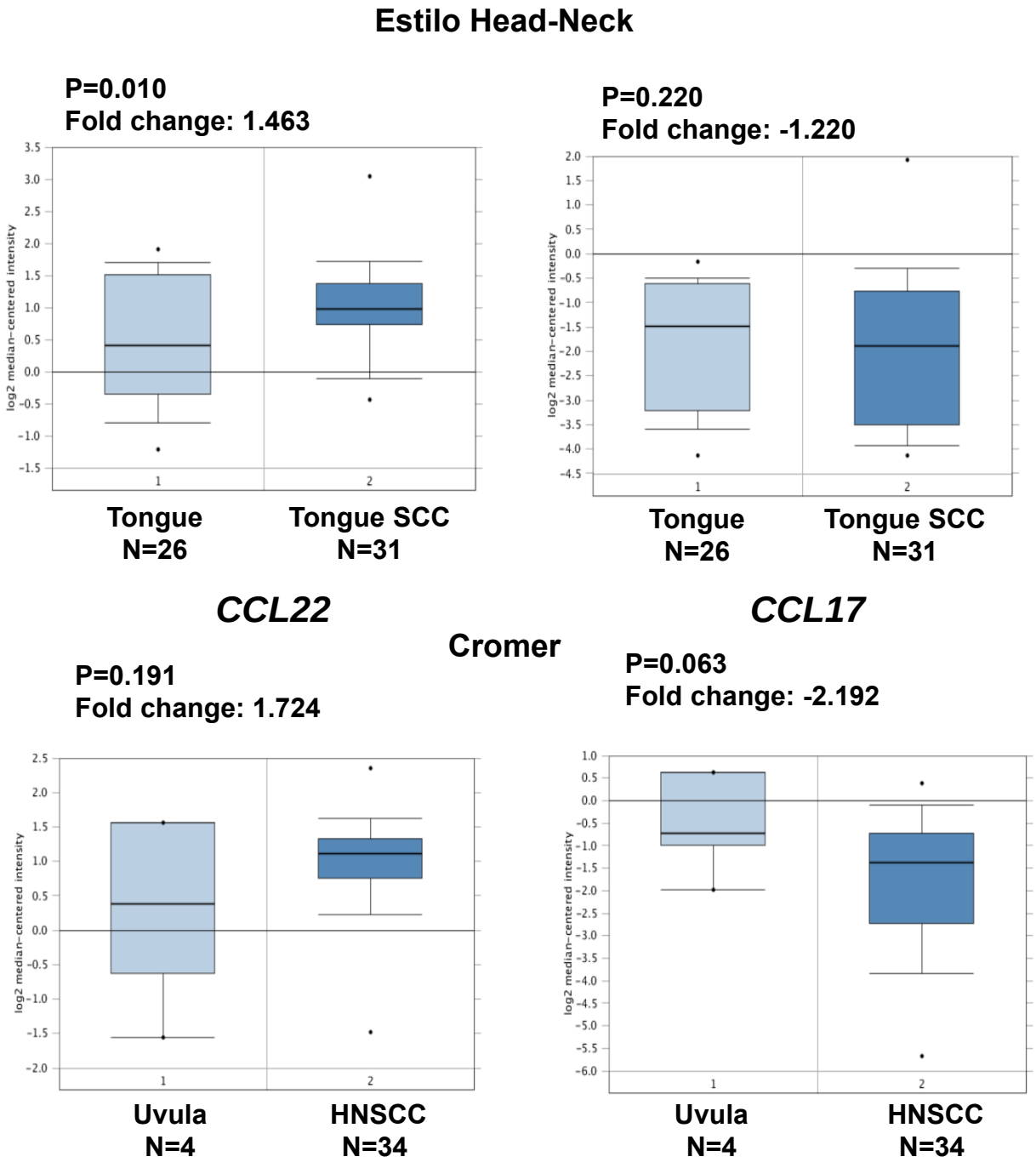

Fold changes and the significance (p-value) are shown on the top of each bar graph

Fig. S2 Little or no significant correlation between *CCL22* expression and the overall and recurrence-free survival

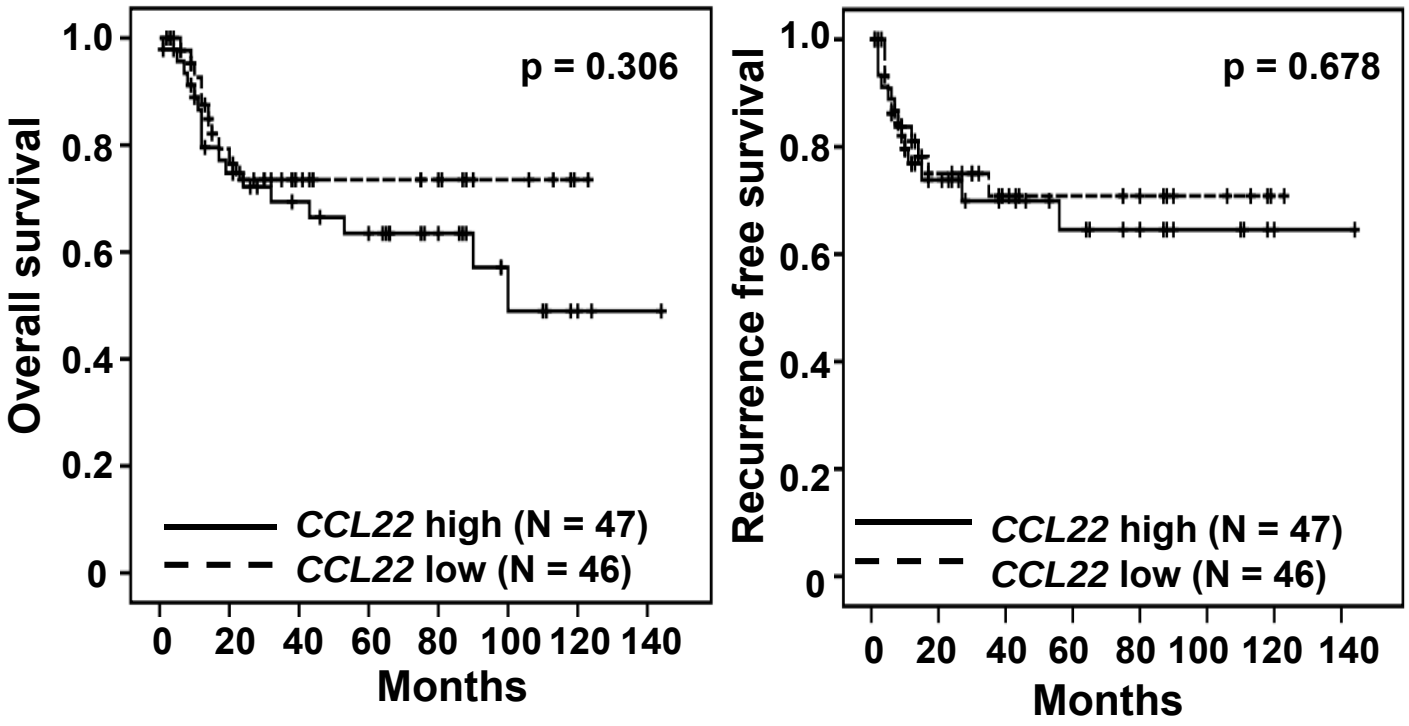

Following qRT-PCR analysis of *CCL22* expression, Kaplan-Meier survival curve analysis for the indicated survival in the 93 oral cancer patients at NCKUH was performed. These patients were stratified into two groups using the median CCL22 mRNA level.

Fig. S3 Differential expression of CCL22 protein in oral cancer cell lines

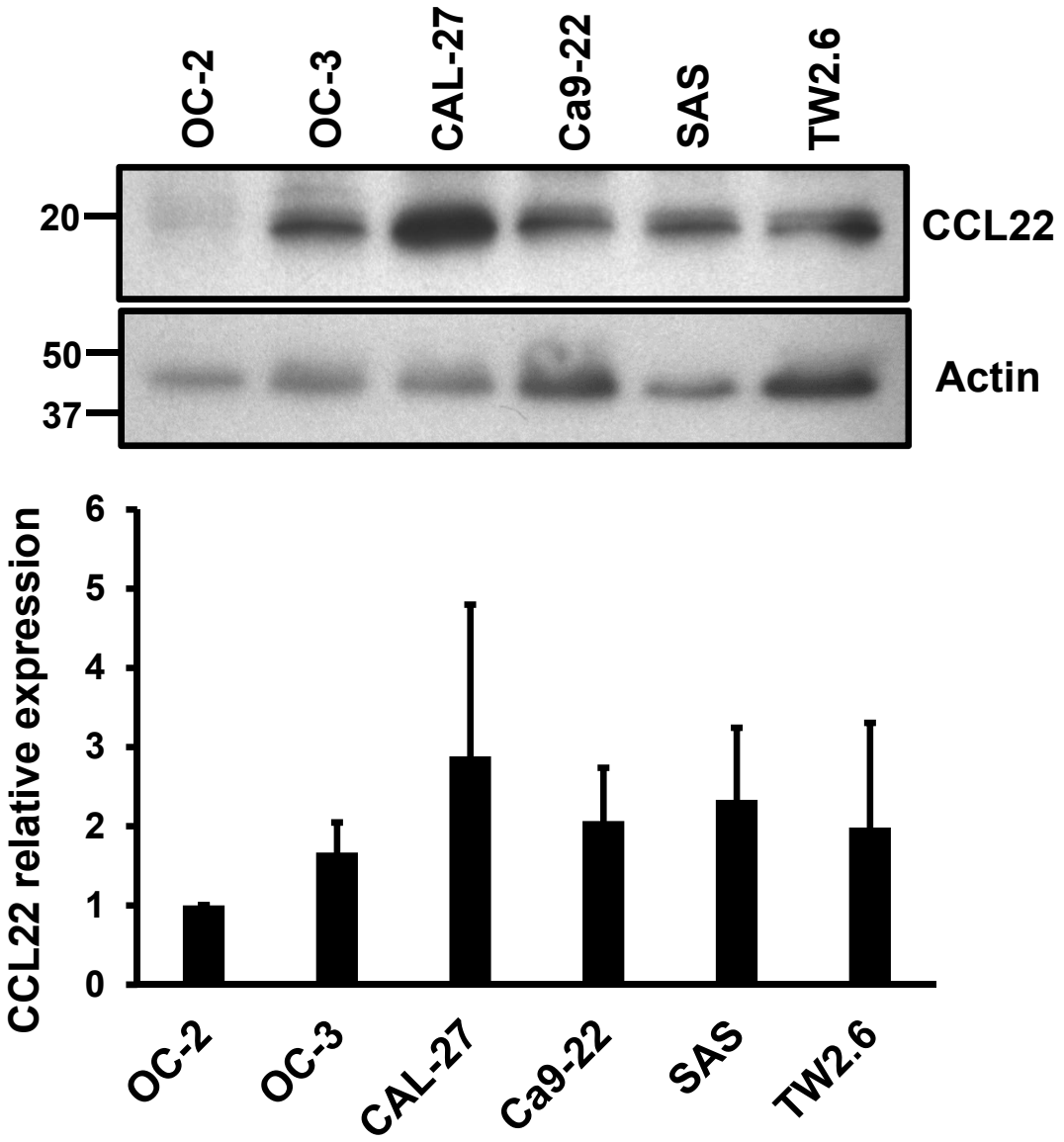

Top: Western blot analysis of CCL22 protein expression in various oral cancer cell lines. Actin serves as an internal loading control. Bottom: The relative levels of CCL22 protein expression in each line relative to OC2 line are shown as Mean SD (N=3).

Fig. S4 The abundance of CCL22 protein in the CM isolated from CCL22-knockdown cells

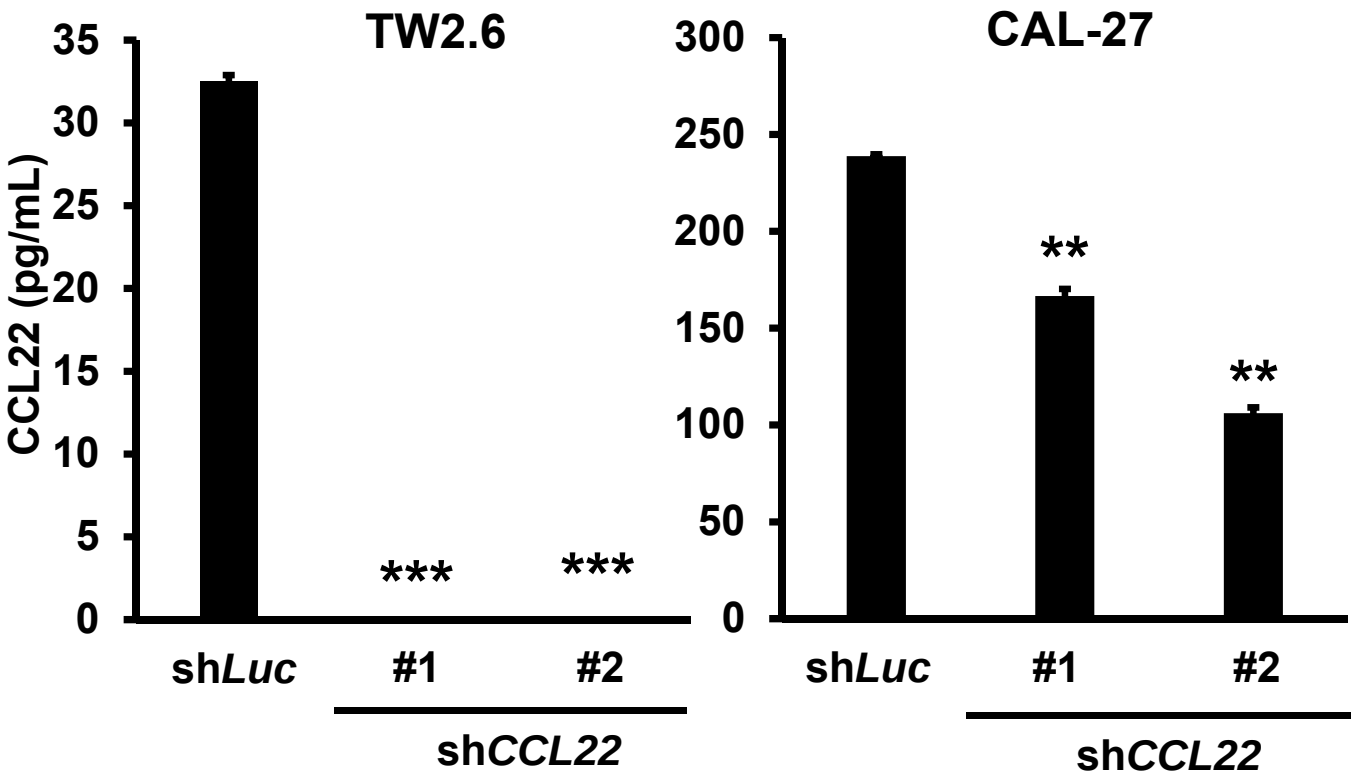

ELISA analysis of CCL22 protein in the serum-free CM harvested from sh*Luc* control or sh*CCL22*-bearing oral cancer cells. **p<0.01 or ***p<0.001 versus sh*Luc*.

Fig. S5 Concordant decrease of Foxp3 mRNA with Ccl22 mRNA expression in Ccl22 knockdown tumor grafts

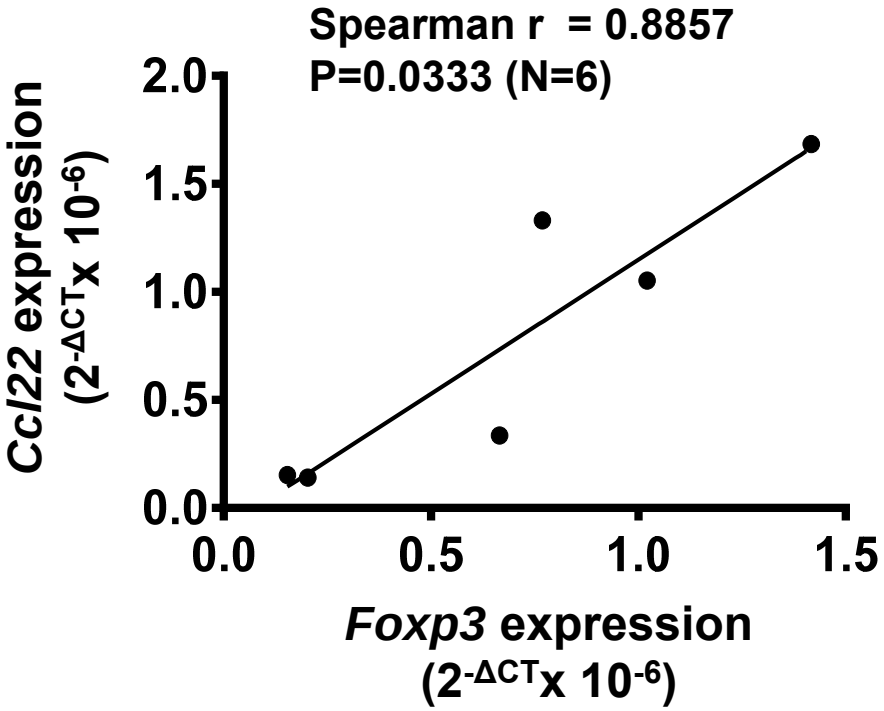

Following RT-qPCR analysis of the *Ccl22* and *Foxp3* mRNA expression in the Ccl22-deRpleted AT84 tumor grafts, Spearman correlation was performed to examine the relation of *Ccl22* and *Foxp3* mRNA expression in the tumors.

Fig. S6 The induction of mouse oral cancer by 4NQO and arecoline

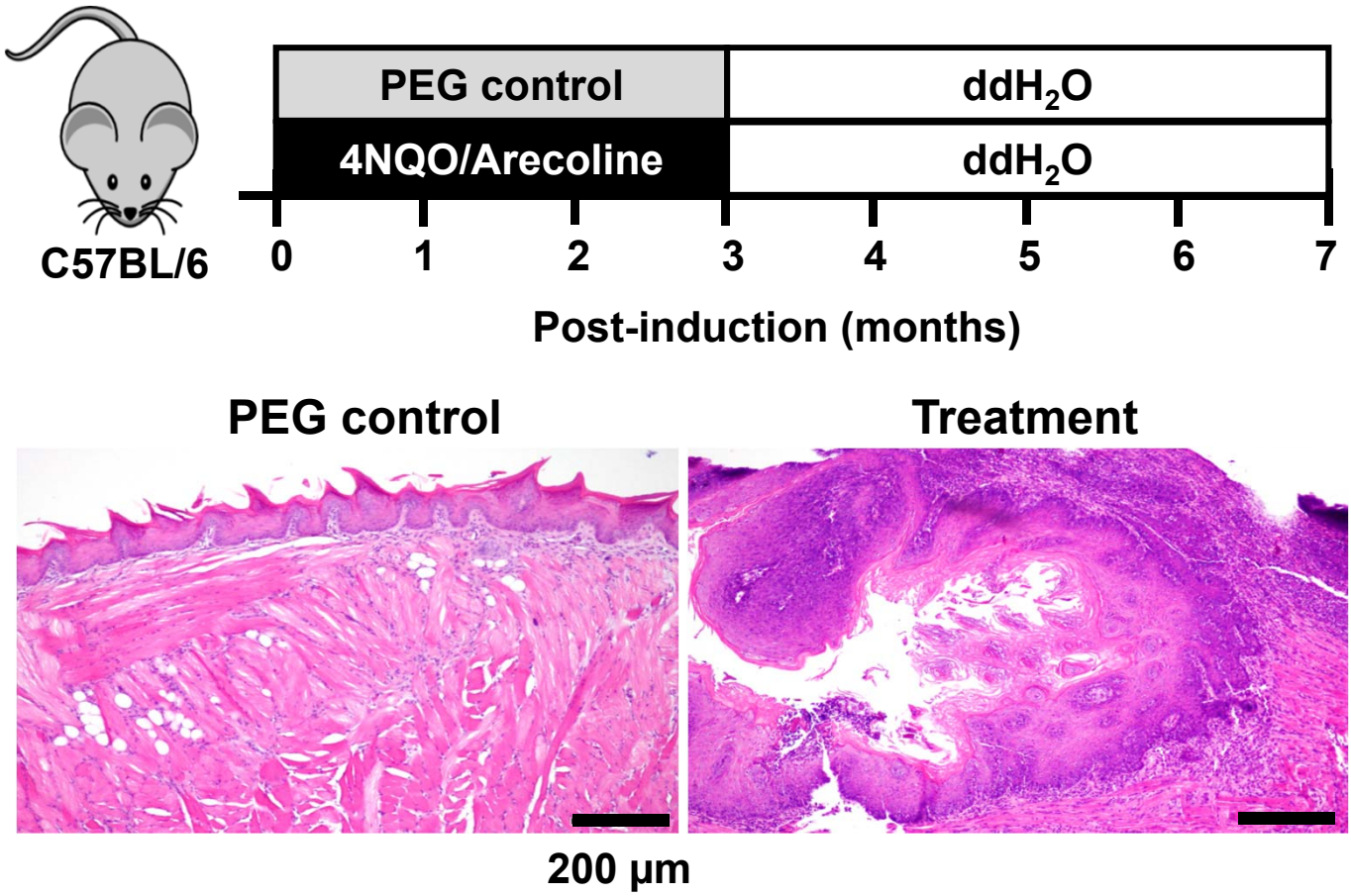

Top, A schematic showing the co-treatment of 4NQO with arecoline or the PEG control. Bottom, H&E staining of representative gross lesions in the control and drug-treated tongue tissues. Scale bar, 200 μm.

Fig. S7 CM derived from CAF-treated oral cancer cells promoted Treg migration and mRNA expression of TGFB, IFNG, and MCP1 in isolated NFs and CAFs derived from clinical specimens

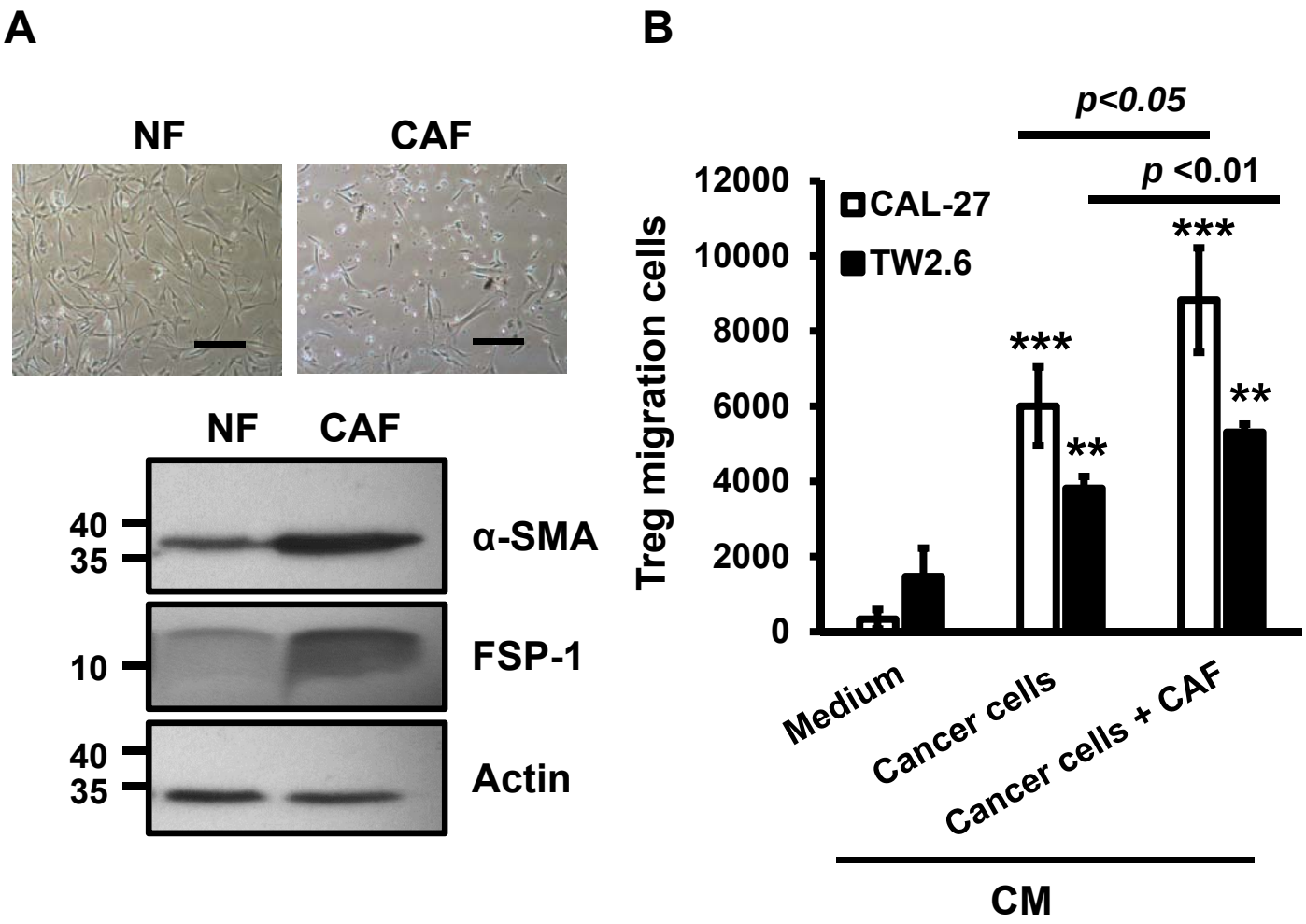

(A) Top, light microscopy under 40X magnification. Scale bar, 200 μm. Bottom, Western blot analysis of α-SMA and FSP-1, two fibroblast markers, in NFs and CAFs. Actin is the internal loading control. (B) The indicated CM from CAF-treated oral cancer cells, CAL-27 or TW2.6, significantly promoted human Treg migration when compared with those treated with NF-treated medium. **p<0.01; ***p<0.001 versus medium alone.

Fig. S7 CM derived from CAF-treated oral cancer cells promoted Treg migration and mRNA expression of TGFB, IFNG, and MCP1 in isolated NFs and CAFs derived from clinical specimens

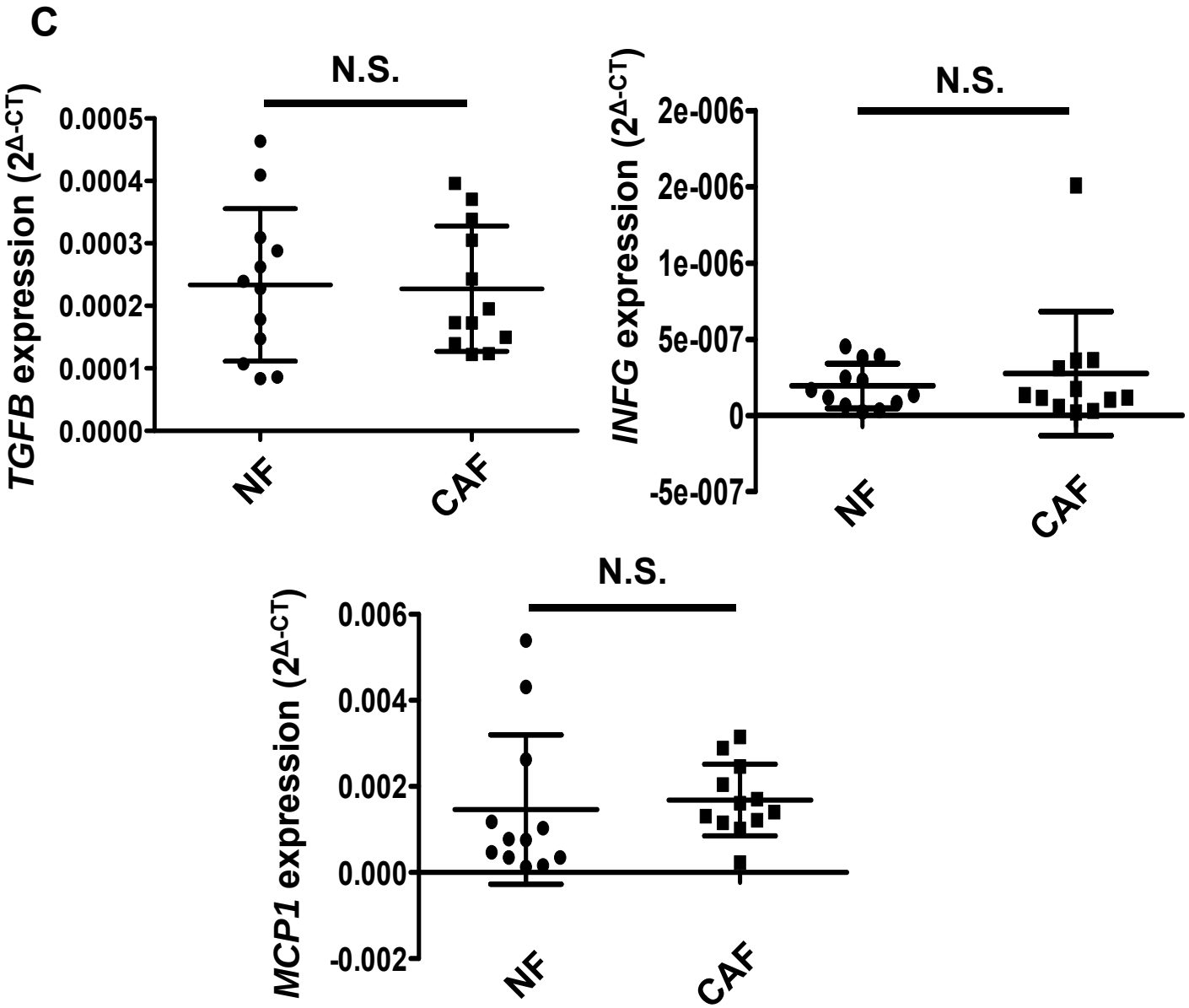

(C)The mRNA levels of *TGFB*, *IFNG,* and *MCP1* in 12 pairs of NFs and CAFs were expressed as Mean+/-SEM. N.S. not significant versus NFs.

Fig. S8 Recombinant IL-1β stimulates CCL22 mRNA expression in oral cancer cells

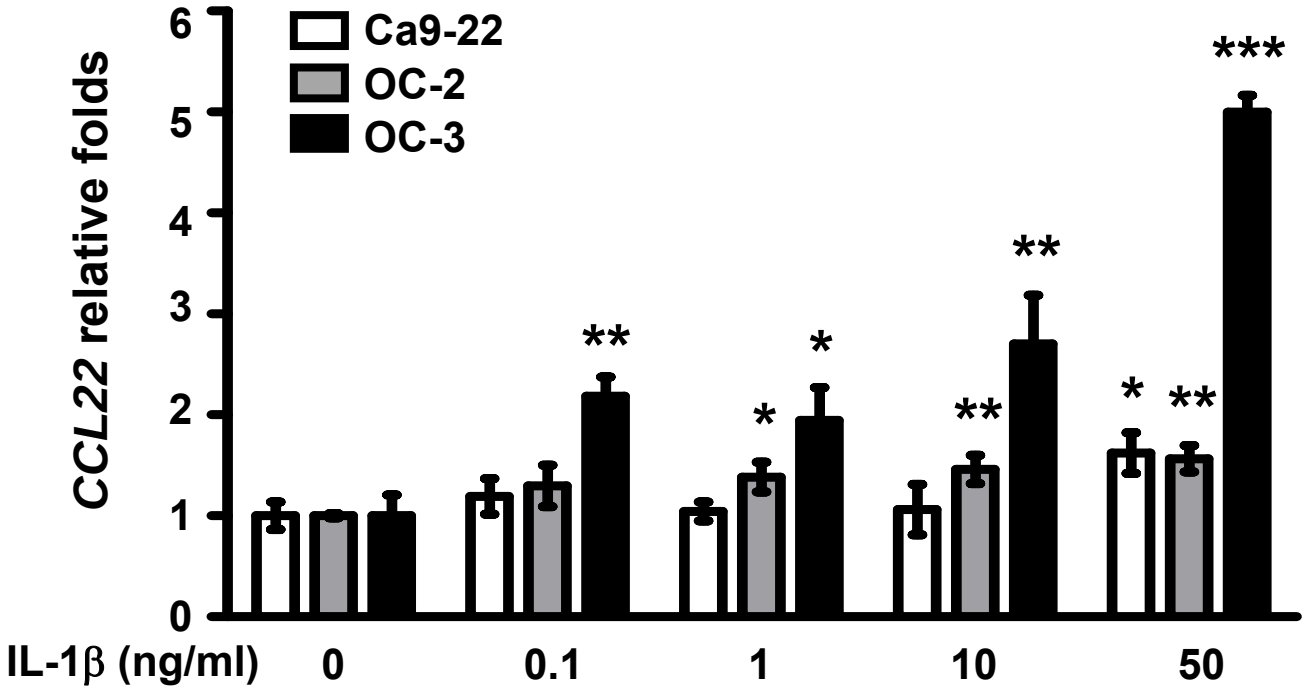

Following the IL-1β treatment for 4 hours at the indicated dose (0.1-50 ng/mL), total RNA were isolated from the treated oral cancer cells, Ca9-22, OC-2 or OC-3, and subjected to RT-qPCR analysis for the expression of *CCL22* mRNA. Actin serves as an internal control. **p*<0.05; ***p*<0.01; ****p*<0.001 versus untreated cells

Fig. S9 The NF-κB subunit, p65 potently induces CCL22 promoter activity

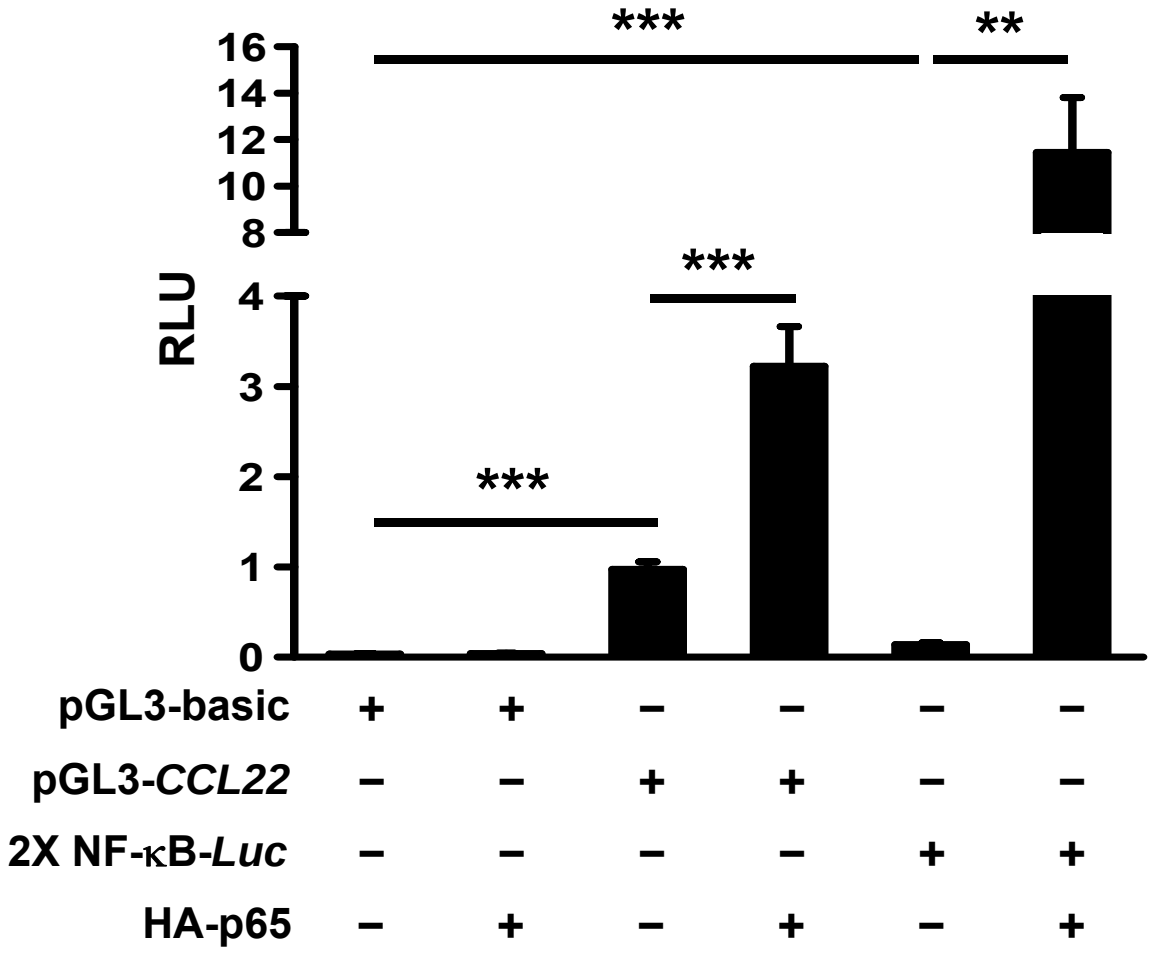

Human oral cancer Ca9-22 cells were transiently transfected with the indicated reporter constructs with the HA vector or an HA-p65 expression vector. 2X NF-κB-Luc with two copies of the p65 binding site upstream of the luciferase (*Luc)* gene was included as a positive control for NF-κB activation. ***p*<0.01; ****p*<0.001 versus pGL3-basic vector control.

Fig. S10 The status of activating phosphorylation of NF-κB proteins in pairwise NFs and CAFs

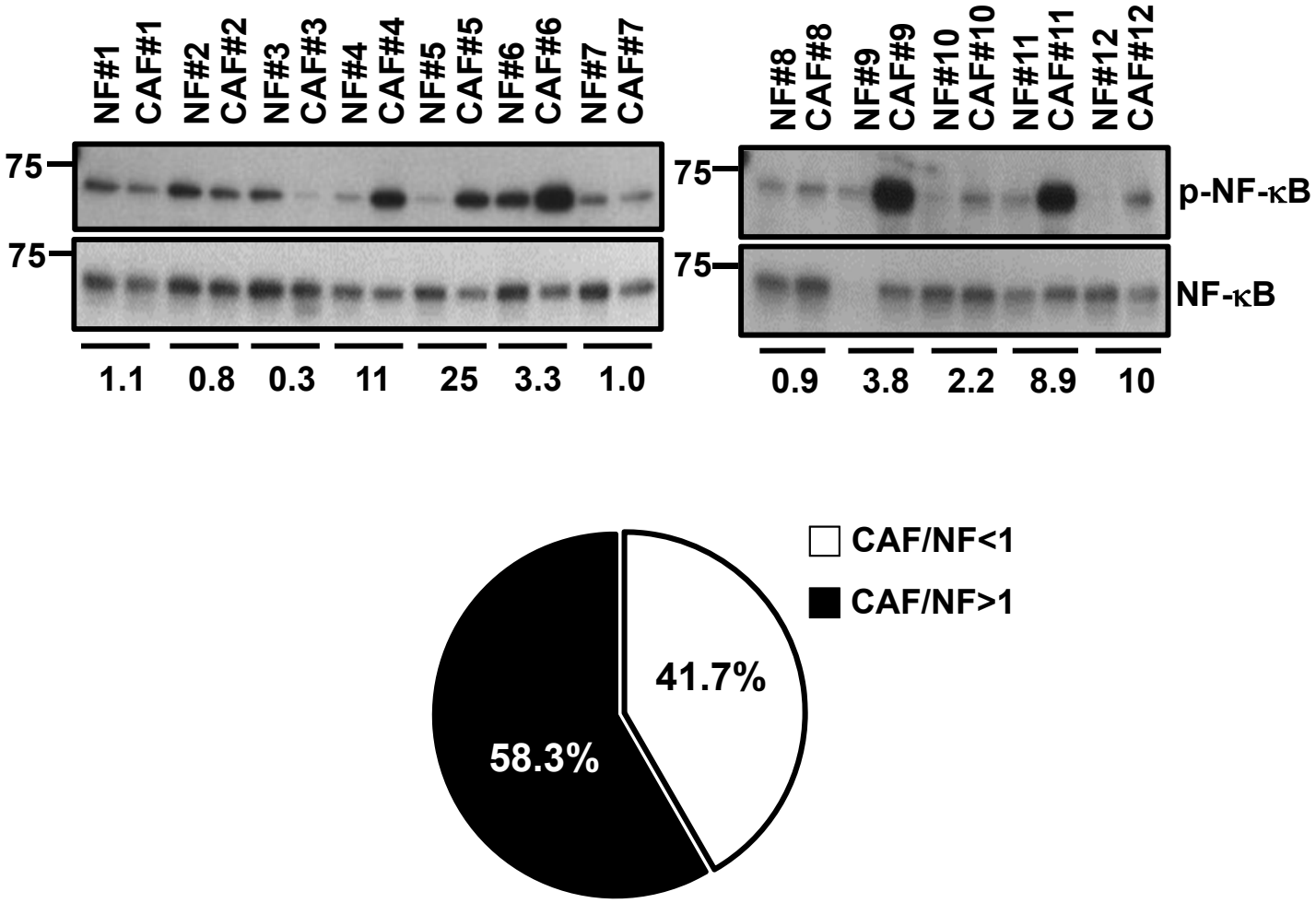

Top: Western blot analysis of activating phosphorylation status (p-NF-κB) and the total level of NF-κB protein in the protein lysates collected from 12 pairs of NFs and CAFs. The numbers underneath each blot are the fold change of activating phosphorylation of NF-κB in each pair of NFs and CAFs. Bottom: the percentage of increase (CAF/NF>1) or decrease (CAF/NF<1) of activating NF-κB phosphorylation in 12 pairs of NFs and CAFs.